AIP Journal of Applied Physics

Subwavelength acoustic focusing by surface-wave-resonance enhanced transmission in doubly negative acoustic metamaterials

Xiaoming Zhou, M. Badreddine Assouar, and Mourad Oudich

Citation: Journal of Applied Physics **116**, 194501 (2014); doi: 10.1063/1.4901996
View online: http://dx.doi.org/10.1063/1.4901996
View Table of Contents: http://scitation.aip.org/content/aip/journal/jap/116/19?ver=pdfcov
Published by the AIP Publishing

JOURNAL OF APPLIED PHYSICS **116**, 194501 (2014)

Subwavelength acoustic focusing by surface-wave-resonance enhanced transmission in doubly negative acoustic metamaterials

Xiaoming Zhou,[1,2] M. Badreddine Assouar,[1,2,a)] and Mourad Oudich[1,2]
[1]*CNRS, Institut Jean Lamour, Vandoeuvre-lès-Nancy F-54506, France*
[2]*Institut Jean Lamour, University of Lorraine, Boulevard des Aiguillettes, BP: 70239, 54506 Vandoeuvre-lès-Nancy, France*

(Received 21 August 2014; accepted 5 November 2014; published online 17 November 2014)

We present analytical and numerical analyses of a yet unseen lensing paradigm that is based on a solid metamaterial slab in which the wave excitation source is attached. We propose and demonstrate sub-diffraction-limited acoustic focusing induced by surface resonant states in doubly negative metamaterials. The enhancement of evanescent waves across the metamaterial slab produced by their resonant coupling to surface waves is evidenced and quantitatively determined. The effect of metamaterial parameters on surface states, transmission, and wavenumber bandwidth is clearly identified. Based on this concept consisting of a wave source attached on the metamaterial, a high resolution of $\lambda/28.4$ is obtained with the optimum effective physical parameters, opening then an exciting way to design acoustic metamaterials for ultrasonic focused imaging. © *2014 AIP Publishing LLC*. [http://dx.doi.org/10.1063/1.4901996]

I. INTRODUCTION

Focused ultrasound is widely used in medical diagnosis as a noninvasive and inexpensive method. Suffered, however, from diffraction of sound, the resolution of a conventional acoustic imaging device is limited to half working wavelength. A most basic approach to increase the resolution is to raise the operating frequency, but at the cost of lowering the penetration depth of ultrasounds. For many decades, it is highly demanded for the resolution of acoustic focusing to be improved without the enhancement of operating frequency. The diffraction limit is caused by the absence in the focusing spot of evanescent waves, which contain deep subwavelength information, due to their rapid decay in the near field. To break the diffraction limit, it is essential for the lens system to enhance evanescent wave amplitude. As a newly emerging field, acoustic metamaterials[1,2] (MTMs) are providing solutions for sub-diffraction-limited resolution by enhancing evanescent waves.[3–5] Designed with the MTM concept, acoustic hyperlens and superlens are two typical kinds of imaging devices capable of evanescent wave manipulation. Acoustic hyperlens is termed for metamaterials with hyperbolic dispersion relation, achieved normally from the concept of anisotropic dynamic mass density.[4–11] The hyperlens prevents evanescent waves from decaying by converting them to propagating waves within the lens, which can then be transferred to the far side of the lens used for the image formation. The converting mechanism relies on the flat dispersion curve with respect to the parallel momentum due to extremely anisotropic mass density. The transferring mechanisms discovered so far include the Fabry-Pérot resonance,[5,7,8] extraordinary transmission at near-zero mass,[10] and the resonant tunneling.[9] Besides above features, "far-field" hyperlens requires additionally the magnifying mechanism by which evanescent waves become propagating ones when they cross the lens.[4,6,12] The best resolution by the hyperlens reported in experiment is $\lambda/50$ (λ is the wavelength).[5] Although the hyperlens is capable of enhancing contrast of subwavelength-size objects from the background, it lacks the ability of ultrasound focusing.

Acoustic superlens has the ability of ultrasonic subwavelength focusing, whose idea can be traced back to the Pendry's perfect lens in optic superfocusing.[13,14] The optic perfect lens is a MTM flat slab with doubly negative (DNG) permittivity and permeability. When an optical source is placed in front of the MTM slab, the emitted propagating waves can converge on the other side of the MTM slab due to negative refraction and evanescent waves can be strongly enhanced by coupling to surface waves supported by MTMs. Thus, the focus can be as sharp as the source due to both the convergence of propagating waves and the recovering of evanescent waves. Acoustic superlens shares the same physics with the optic one.[15] Furthermore, there is an analogy in the surface wave condition between fluid MTMs with trivial shear modulus and optical ones. In view of biomedical imaging applications, the structure models of the no-shear fluid MTMs recently proposed are not suitable for the human tissue environment, while serve mainly for the air environment.[16–20] In contrast, solid MTMs[21] are found to be good candidates for acoustic wave manipulation in dense liquids, for example, used for subwavelength focusing in mercury.[22] Various structure models of solid metamaterials relying on the chiral effect or the resonance of multiple inclusions have been proposed.[23–26] It has been demonstrated with numerical analyses that the solid DNG MTMs[23,24] have nearly the water impedance, and thus are more suitably used in biomedical environment. The main physical difference between fluid and solid MTMs is the presence of shear waves for the latter material. Up to now, the physics of acoustic focused imaging by general solid MTMs and the influence of the shear modulus on the resolution are not clearly discovered.

[a)]Author to whom correspondence should be addressed. Electronic mail: Badreddine.Assouar@univ-lorraine.fr

In this work, we propose and demonstrate analytically and numerically sub-diffraction-limited acoustic focusing, induced by surface resonant states of DNG MTMs, with potential applications to acoustic high-resolution imaging. Figure 1 illustrates the analyzed model, which consists in a MTM flat slab of thickness d sandwiched between two different fluid half-spaces. The left half-space is the source region, where the air environment is considered and a small ultrasonic transducer would be attached to the MTM surface in practical application as the wave source. Subwavelength ultrasound focusing will be generated in the right half-space, where the water is employed to simulate the human tissue environment due to their similar acoustic characteristics. In Sec. II, we analyze surface wave conditions for the special case of no-shear fluid MTMs, for later comparison study with the general solid ones. In the Secs. III and IV, surface wave conditions and wave propagation characteristics of solid MTMs will be analyzed, and the influence of the MTM's parameters on surface states and transmission will be studied. High-resolution acoustic focusing by solid MTMs will be designed and verified by full-wave numerical simulation in Sec. V.

II. SURFACE RESONANT STATES IN NO-SHEAR FLUID METAMATERIALS

Assume the mass density ρ and bulk modulus κ for the fluid MTM, both of which can be negative values. The mass density and sound velocity are, respectively, $\rho_A = 1.25\,\mathrm{kg/m^3}$ and $c_A = 343\,\mathrm{m/s}$ for the air, and $\rho_W = 1000\,\mathrm{kg/m^3}$ and $c_W = 1490\,\mathrm{m/s}$ for the water. Their bulk modulus can be computed by $\kappa_A = \rho_A c_A^2$ and $\kappa_W = \rho_W c_W^2$. Without loss of generality, we assume two-dimensional scenario in which wave fields depend only on the propagation direction x and one transverse coordinate y. Let us seek conditions for surface waves existing at interfaces between MTMs and fluids. The criterion for surface waves is that the wave fields decay exponentially in the direction perpendicular to the interface. Thereby, the pressure p and displacement field u in the direction x for each region of the system can be written as

$$p = a_1 e^{q_A x} e^{ik_s y}, \tag{1}$$

$$u = \frac{q_A}{\rho_A \omega^2} a_1 e^{q_A x} e^{ik_s y}, \tag{2}$$

for the region $x \le 0$,

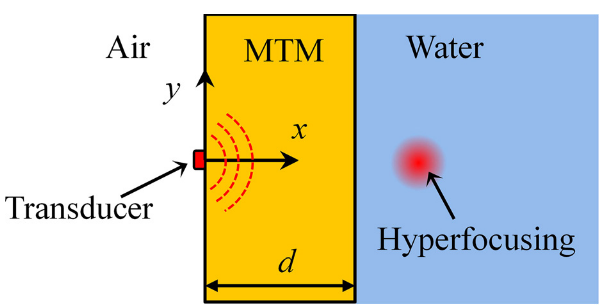

FIG. 1. Schematic view of the lensing model made up of a MTM flat slab in which the wave excitation source is attached.

$$p = (b_1 e^{-q_F x} + b_2 e^{q_F x}) e^{ik_s y}, \tag{3}$$

$$u = \frac{q_F}{\rho \omega^2}(-b_1 e^{-q_F x} + b_2 e^{q_F x}) e^{ik_s y}, \tag{4}$$

for the region $0 \le x \le d$, and

$$p = a_2 e^{-q_W (x-d)} e^{ik_s y}, \tag{5}$$

$$u = \frac{-q_W}{\rho_W \omega^2} a_2 e^{-q_W (x-d)} e^{ik_s y}, \tag{6}$$

for the region $x \ge d$, where k_s is the wave number of the surface wave to be determined. The wave numbers of evanescent waves in the air, the water, and the fluid MTMs are, respectively, $q_A = \sqrt{k_s^2 - \omega^2/c_A^2}$, $q_W = \sqrt{k_s^2 - \omega^2/c_W^2}$, and $q_F = \sqrt{k_s^2 - \omega^2 \rho/\kappa}$. The time harmonics $\exp(-i\omega t)$ has been assumed. Continuous conditions of pressures and displacements at interfaces $x = 0$ and $x = d$ result in four equations for the constants a_1, b_1, b_2, and a_2. A nontrivial solution of these equations exists if the determinant of the coefficients of four constants vanishes, which yields the following dispersion equation:

$$\frac{\rho_A}{q_A}\left[\frac{q_W}{\rho_W}\left(1+Q_F^2\right)+\frac{q_F}{\rho}\left(1-Q_F^2\right)\right] + \frac{\rho}{q_F}\left[\frac{q_W}{\rho_W}\left(1-Q_F^2\right)+\frac{q_F}{\rho}\left(1+Q_F^2\right)\right] = 0, \tag{7}$$

where $Q_F = e^{-q_F d}$.

Let us first visit two special cases. When the two half-spaces are both water, the dispersion equation for the water/MTM/water system is

$$\frac{q_W}{\rho_W}(1 \pm Q_F) + \frac{q_F}{\rho}(1 \mp Q_F) = 0. \tag{8}$$

When the infinite thickness of the metamaterial slab, i.e., $Q_F \ll 1$, is considered in Eq. (8), which means the decoupling between two interfaces, the dispersion equation for the MTM/water system becomes[15]

$$\frac{q_W}{\rho_W} + \frac{q_F}{\rho} = 0. \tag{9}$$

For the studied model, where the left half-space is air and the right one is water, a reasonable simplification can be made for Eq. (7) based on the fact that $\rho_A \ll |\rho|, \rho_W$. Thereby, the first term in Eq. (7) can be neglected, resulting in a more simple form

$$\frac{q_W}{\rho_W}\left(1-Q_F^2\right) + \frac{q_F}{\rho}\left(1+Q_F^2\right) = 0. \tag{10}$$

This simplification is equivalent to the traction-free boundary condition $p = 0$ imposed at the interface $x = 0$. Such condition together with continuous conditions of pressures and displacements at interface $x = d$ lead to three equations for the constants b_1, b_2, and a_2. The vanishing determinant of the corresponding coefficient matrix yields the same result to Eq. (10).

For the existence of surface waves, it is required that $k_s^2 > \omega^2/c_W^2$ and $k_s^2 > \omega^2\rho/\kappa$, which means q_W, $q_F > 0$ and $0 < Q_F < 1$. Then, the necessary condition for the presence of surface waves is the negative density ($\rho < 0$) of MTMs, which is true for the water/MTM/water, MTM/water, and air/MTM/water systems, as verified by Eqs. (8), (9), and (10), respectively. For the studied model, the condition $k_s^2 > \omega^2/c_A^2$ is not necessary. Without this condition, surface waves exist only at the MTM-water interface, instead of the air-MTM one.

For plane acoustic waves with parallel wave number k_y incident leftwards on the MTM slab, the pressure and displacement field in each region of the system are expressed as

$$p = (A_0 e^{ik_A x} + A_1 e^{-ik_A x})e^{ik_y y}, \tag{11}$$

$$u = \frac{ik_A}{\rho_A \omega^2}\left(A_0 e^{ik_A x} - A_1 e^{-ik_A x}\right)e^{ik_y y}, \tag{12}$$

for the region $x \le 0$,

$$p = (B_1 e^{ik_F x} + B_2 e^{-ik_F x})e^{ik_y y}, \tag{13}$$

$$u = \frac{ik_F}{\rho \omega^2}\left(B_1 e^{ik_F x} - B_2 e^{-ik_F x}\right)e^{ik_y y}, \tag{14}$$

for the region $0 \le x \le d$, and

$$p = A_2 e^{ik_W(x-d)}e^{ik_y y}, \tag{15}$$

$$u = \frac{ik_W}{\rho_W \omega^2} A_2 e^{ik_W(x-d)}e^{ik_y y}, \tag{16}$$

for the region $x \ge d$, where $k_A = \sqrt{\omega^2/c_A^2 - k_y^2}$, $k_W = \sqrt{\omega^2/c_W^2 - k_y^2}$, and $k_F = \sqrt{\omega^2\rho/\kappa - k_y^2}$. By use of continuous boundary conditions, transmission coefficients $T = A_2/A_0$ are derived to be

$$T = \frac{4e^{ik_F d}}{\frac{\rho_A}{k_A}\left[\frac{k_W}{\rho_W}(1 + e^{2ik_F d}) + \frac{k_F}{\rho}(1 - e^{2ik_F d})\right] + \frac{\rho}{k_F}\left[\frac{k_W}{\rho_W}(1 - e^{2ik_F d}) + \frac{k_F}{\rho}(1 + e^{2ik_F d})\right]}. \tag{17}$$

By comparison of Eqs. (7) and (17), it is readily found that the denominator of Eq. (17) vanishes when the parallel wavenumber of incident waves k_y matches the wavenumber k_s of surface waves. Transmission coefficients reach infinity in this case, meaning that evanescent waves can be resonantly enhanced in amplitudes when they cross the MTM slab. This is the main idea for superlens to achieve acoustic subwavelength focusing beyond the diffraction limit. For three systems mentioned above, there all exist the perfect imaging condition, i.e., $\rho = -\rho_W$ and $\kappa = -\kappa_W$, which means that any value of k_s is solution of dispersion equations. Therefore, perfect focusing is expected from this condition, as all components of evanescent waves can be recovered by coupling to surface waves of MTMs.

For further study, Figure 2 displays the pressure field amplitudes along the line $y = 0$ of the air/MTM/water and water/MTM/water systems under disturbance of acoustic waves with the parallel wavenumber $k_y = 3.55\omega/c_W$. Note that the MTM occupies the region between 0 and $x/d = 1$. The parameters of the MTM slab are $\rho = -0.99\rho_W$, $\kappa = -0.8\kappa_W$, and $d = 20$ mm, and the operating frequency is chosen as 30 kHz, which will be also used for all other examples presented in this work. For clear illustration, the pressure distribution has been normalized to the values at $|p(x=0)|$ in either system. It is observed that the ratio of pressure fields $|p(x=d)|/|p(x=0)|$ across the MTM slab is beyond the unity, demonstrating clearly the enhancement effect of evanescent waves. For the air/MTM/water system, acoustic wave can still propagate in the air region because of the smaller wave velocity than in the water, and so surface waves are excited only at the interface $x = d$. Surprisingly, the pressure amplitude ratios across the MTM slab are exactly the same for both systems. For theoretical verification, we define the transfer function (TF) as the pressure ratio $p(x=d)/p(x=0)$, which can be derived as

$$TF = \frac{2k_F \rho_W e^{ik_F d}}{k_W \rho(1 - e^{2ik_F d}) + k_F \rho_W (1 + e^{2ik_F d})}. \tag{18}$$

It is indeed the fact that the transfer function is unrelated to physical properties of the incident region (i.e., the back

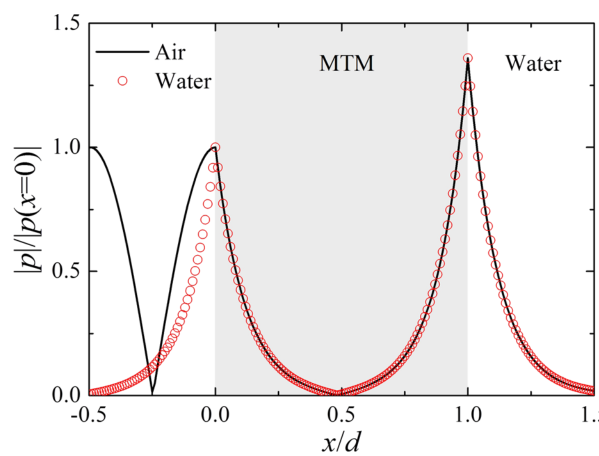

FIG. 2. Pressure amplitude distribution along the line $y = 0$ in both the air/MTM/water and water/MTM/water systems for acoustic wave with the parallel wavenumber $k_y = 3.55\omega/c_W$ and operating frequency 30 kHz. The parameters of the MTM slab are $\rho = -0.99\rho_W$, $\kappa = -0.8\kappa_W$, and $d = 20$ mm.

medium). This also reveals the superiority of the proposed superlens model, in that the enhancement effect of evanescent waves is invariant to the back medium when the source is attached to the MTM surface. After a clear understanding of the surface resonant states and associated enhancement effect in the fluid MTM case, we will examine in Sec. III the surface states enabled by solid MTMs.

III. SURFACE RESONANT STATES IN SOLID METAMATERIALS

We assume that the solid MTM is characterized by mass density ρ and Lamé coefficients λ and μ. Following the criterion for surface waves, the displacement in the direction x, the normal and shear stresses in the MTM region are expressed, respectively, as

$$u = \left(\frac{iq_L}{k_s} b_1 e^{-q_L x} + \frac{ik_s}{q_T} b_2 e^{-q_T x} - \frac{iq_L}{k_s} b_3 e^{q_L x} - \frac{ik_s}{q_T} b_4 e^{q_T x}\right) e^{ik_s y}, \tag{19}$$

$$\sigma_{xx} = \left\{\left[i\lambda k_s - i(\lambda+2\mu)\frac{q_L^2}{k_s}\right](b_1 e^{-q_L x} + b_3 e^{q_L x}) - 2i\mu k_s (b_2 e^{-q_T x} + b_4 e^{q_T x})\right\} e^{ik_s y}, \tag{20}$$

$$\sigma_{xy} = \left[2\mu q_L(-b_1 e^{-q_L x} + b_3 e^{q_L x}) + \mu\left(q_T + \frac{k_s^2}{q_T}\right)(-b_2 e^{-q_T x} + b_4 e^{q_T x})\right] e^{ik_s y}, \tag{21}$$

where $q_L = \sqrt{k_s^2 - \omega^2\rho/(\lambda+2\mu)}$ and $q_T = \sqrt{k_s^2 - \omega^2\rho/\mu}$ are, respectively, wave numbers of longitudinal and transverse evanescent waves in the solid MTMs. For the studied model, one can get five equations for the constants b_1, b_2, b_3, b_4, and a_2 by using the traction-free boundary condition, namely $\sigma_{xx} = \sigma_{xy} = 0$, at the interface $x = 0$, in conjunction with continuous conditions of normal stress and displacements as well as the zero-shear-stress condition at interface $x = d$. The dispersion equation of surface waves can be obtained by the vanishing determinant of the corresponding coefficient matrix. The dispersion relation is too tedious to be shown here. However, there exists an efficient simplification, as will be presented below.

To proceed, the dispersion equation for the MTM/water system will be given first. The stress and displacement fields in the MTM half-space are written as

$$u = \left(-\frac{iq_L}{k_s} b_1 e^{q_L x} - \frac{ik_s}{q_T} b_2 e^{q_T x}\right) e^{ik_s y}, \tag{22}$$

$$\sigma_{xx} = \left\{\left[i\lambda k_s - i(\lambda+2\mu)\frac{q_L^2}{k_s}\right] b_1 e^{q_L x} - 2i\mu k_s b_2 e^{q_T x}\right\} e^{ik_s y}, \tag{23}$$

$$\sigma_{xy} = \left[2\mu q_L b_1 e^{q_L x} + \mu\left(q_T + \frac{k_s^2}{q_T}\right) b_2 e^{q_T x}\right] e^{ik_s y}. \tag{24}$$

Consider the fluid-solid interfacial conditions by use of Eqs. (5), (6), and (22)–(24). The dispersion equation of surface waves for the MTM/water system is

$$\rho_W q_L + \rho q_W = \frac{2\mu q_W k_s^2}{\omega^2} + \frac{2\rho_W q_L k_s^2}{q_T^2 + k_s^2}\left(1 - \frac{2\mu q_T q_W}{\rho_W \omega^2}\right). \tag{25}$$

Note first that the dispersion equation (9) of the fluid MTM/water system can be recovered from Eq. (25) with the parameter $\mu = 0$. To examine the effect of the shear modulus, we assume equal longitudinal wave velocities for the MTM and water, namely $(\lambda+2\mu)/\rho = \kappa_W/\rho_W$, which means $q_L = q_W$. When μ are very small nonzero values, the right-hand side of Eq. (25) must be positive, meaning that $\rho + \rho_W > 0$. $\rho + \rho_W = 0$ is unachievable, since Eq. (25) becomes $q_T = q_W$ in this case, which is never satisfied. To quantify the range of values of μ, we consider the special case where the second term in the right-hand side of Eq. (25) vanishes, i.e.,

$$\rho_W \omega^2 - 2\mu q_T q_W = 0. \tag{26}$$

Equation (25) then becomes

$$\rho_W q_L + \rho q_W = \frac{2\mu q_W k_s^2}{\omega^2}. \tag{27}$$

By combining Eqs. (26) and (27), we get a simple expression for the shear modulus

$$\mu = \frac{\kappa_W}{4(\delta^2 - 1)}, \tag{28}$$

where we have defined the normalized wavenumber δ as $\delta = k_s/(\omega/c_W)$. As an example of a moderate value $\delta = 5$, we can deduce from Eq. (28) that the shear modulus of the MTM is approximately a hundred times lower than the modulus of the water, $\mu = \kappa_W/96$. There is no special meaning for the condition in Eq. (26); in this example, Eq. (26) means the MTM density $-739.6\,\mathrm{kg/m^3}$, Eq. (28) reads an important conclusion: high wavenumbers of surface waves are available in the low-shear-modulus (LSM) medium. Note that $|\lambda| \approx \kappa_W$ in the LSM case; then, the LSM approximation means $\mu \ll |\lambda|$ for high values of δ. In order for further verification of LSM approximation, Figure 3 displays the values of δ at various shear modulus μ of the MTM slab with thicknesses $d = 20$ mm and $d = 10$ mm for both air/MTM/water and MTM/water systems. Two different MTM densities $\rho = -950$ and $-990\,\mathrm{kg/m^3}$ are considered and parameters of the modulus satisfy $(\lambda+2\mu)/\rho=\kappa_W/\rho_W$. It is clearly illustrated that the shear modulus is indeed much less than $|\lambda|$ and κ_W for high values of δ, confirming the validity of the LSM approximation.

Under the LSM approximation, we can simplify the dispersion equation of surface waves for the air/MTM/water system as

$$q_W\Gamma(1-Q_L^2)+q_L(1+Q_L^2)=0, \tag{29}$$

where it has been defined that $Q_L=e^{-q_Ld}$ and

$$\Gamma(k_s)=(\rho\omega^2-2\mu k_s^2)^2/(\rho\rho_W\omega^4). \tag{30}$$

If $\mu=0$, Eq. (29) can be reduced as expected to the dispersion equation (10). To check the effect of the shear modulus, we consider $q_L=q_W$ and neglect Q_L. Equation (29) results in

$$\delta=\frac{\rho+\sqrt{|\rho|\rho_W}}{2\rho_W}\frac{\kappa_W}{\mu}. \tag{31}$$

From Eq. (31), we can find the way to achieve high wavenumber of surface waves, which is essential in high resolution of subwavelength acoustic focusing, because evanescent waves carrying finer sub-wavelength information can be recovered. The approach of attaining this goal is to either lower the shear modulus or enhance the contrast between $|\rho|$ and ρ_W. Note that for positive δ, it is required that $|\rho|<\rho_W$. In Fig. 3, it is also shown the LSM-approximated results computed by Eq. (30) and a good agreement between exact (numerical) and approximate results can be found. There are minor changes between curves in Figs. 3(a) and 3(b), demonstrating the insensitive dependence of wavenumbers δ on the MTM thickness. Numerical analysis shown in Fig. 3 confirms also that lowering the shear modulus or increasing the contrast between $|\rho|$ and ρ_W can efficiently enhance the wavenumber of surface waves. In Sec. IV, we will examine the enhancement effect of evanescent wave transmission induced by surface resonant states of solid MTMs.

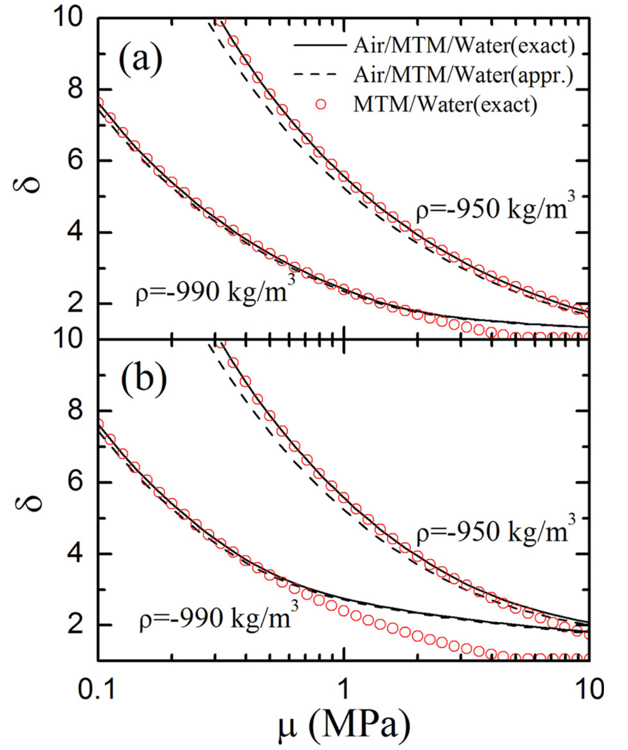

FIG. 3. The normalized wavenumber δ of surface waves enabled by solid MTMs with thicknesses 20 mm (a) and 10 mm (b) for various shear modulus μ, and mass densities in both air/MTM/water and MTM/water systems. The MTM parameters satisfy $(\lambda+2\mu)/\rho=\kappa_W/\rho_W$.

IV. WAVE TRANSMISSION PROPERTIES IN SOLID METAMATERIALS

For an acoustic wave incident on the solid MTM slab, the displacement and stress fields in the MTM are written as

$$u=\left(\frac{k_L}{k_y}B_1e^{ik_Lx}-\frac{k_y}{k_T}B_2e^{ik_Tx}-\frac{k_L}{k_y}B_3e^{-ik_Lx}+\frac{k_y}{k_T}B_4e^{-ik_Tx}\right)e^{ik_yy}, \tag{32}$$

$$\sigma_{xx}=\left\{\left[i\lambda k_y+i(\lambda+2\mu)\frac{k_L^2}{k_y}\right]\left(B_1e^{ik_Lx}+B_3e^{-ik_Lx}\right)-2i\mu k_y\left(B_2e^{ik_Tx}+B_4e^{-ik_Tx}\right)\right\}e^{ik_yy}, \tag{33}$$

$$\sigma_{xy}=\left[2i\mu k_L\left(B_1e^{ik_Lx}-B_3e^{-ik_Lx}\right)+i\mu\left(k_T-\frac{k_y^2}{k_T}\right)\left(B_2e^{ik_Tx}-B_4e^{-ik_Tx}\right)\right]e^{ik_yy}, \tag{34}$$

where $k_L=\sqrt{\omega^2\rho/(\lambda+2\mu)-k_s^2}$ and $k_T=\sqrt{\omega^2\rho/\mu-k_s^2}$. By use of the fluid-solid coupling conditions at interfaces $x=0$ and $x=d$ (see Fig. 1), based on Eqs. (11), (12), (15), (16), and (32)–(34), all unknown scattering coefficients can be uniquely determined. Same to the fluid MTM system, it can also be demonstrated by rigorous theoretical derivation that the transfer function of the solid MTM is unrelated to physical properties of the back medium. Under the LSM approximation, the transfer function can be simplified as

$$TF=\frac{2k_Le^{ik_Ld}}{k_W\Gamma(k_y)(1-e^{2ik_Ld})+k_L(1+e^{2ik_Ld})}. \tag{35}$$

In Eq. (35), the denominator vanishes when k_y is equal to the wavenumber k_s that satisfies the simplified Eq. (29). As a result of this coupling, the transmission profile in the k_y space will be non-uniform, with the infinitely large values at the coupling wavenumber $k_y=k_s$, and gradually decreasing

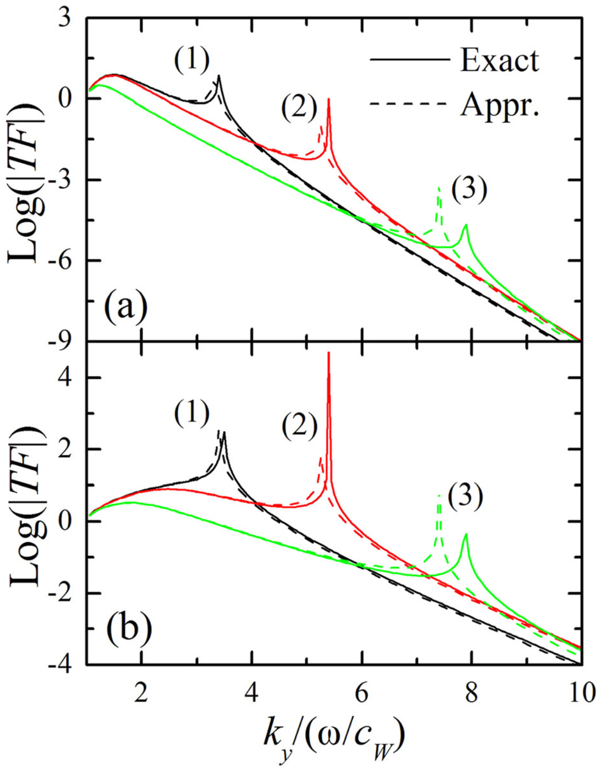

FIG. 4. Amplitudes of transfer function of the solid MTMs with thicknesses 20 mm (a) and 10 mm (b) in three selected cases in Fig. 3: (1) $\rho = -990\,\text{kg/m}^3$ and $\mu = 0.5\,\text{MPa}$; (2) $\rho = -990\,\text{kg/m}^3$ and $\mu = 0.2\,\text{MPa}$; (3)$\rho = -950\,\text{kg/m}^3$ and $\mu = 0.5\,\text{MPa}$.

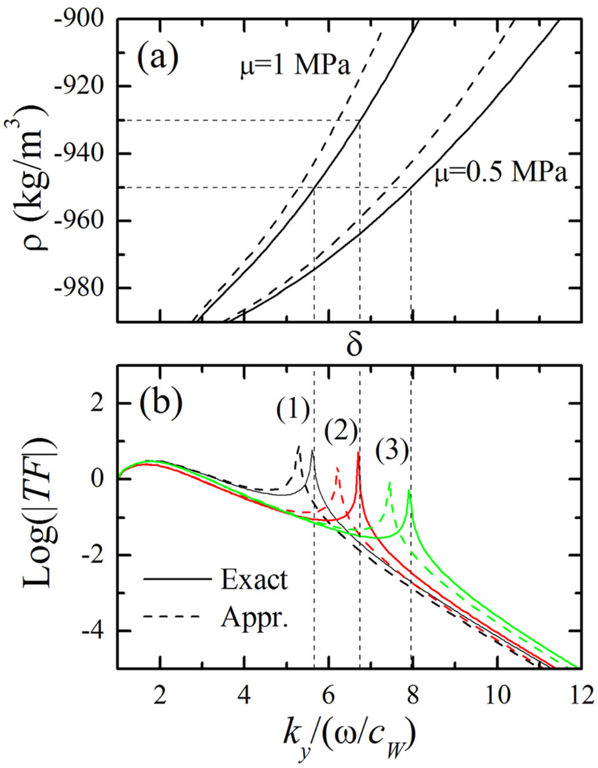

FIG. 5. (a) The normalized wavenumber δ of surface waves enabled by solid MTMs with the thickness $d = 10\,\text{mm}$, shear modulus $\mu = 0.5$ and 1 MPa, and various density ρ, and the modulus of the MTM satisfies $\lambda + 2\mu = -\kappa_W$. (b) Amplitudes of transfer function of the solid MTMs in three selected cases: (1) $\rho = -950\,\text{kg/m}^3$ and $\mu = 1\,\text{MPa}$; (2) $\rho = -930\,\text{kg/m}^3$ and $\mu = 1\,\text{MPa}$; (3) $\rho = -950\,\text{kg/m}^3$ and $\mu = 0.5\,\text{MPa}$.

finite values as k_y away from k_s. To attain the transmission gain (with the TF amplitude greater than (1) in a wider range of k_y, the flatter transmission peak is preferred. In the simplified case where we consider $q_L = q_W$ and neglect $e^{2ik_L d}$ (which is minor for large values of δ) in the denominator of Eq. (35), the wavenumber bandwidth (WNBW) of the transmission gain can be qualitatively evaluated by the following expression:

$$\frac{1}{\text{WNBW}} \propto \left| \frac{d(\Gamma+1)}{dk_y} \bigg|_{\Gamma(k_y)+1=0} \right| = \frac{8\mu k_s}{\omega^2 \sqrt{|\rho\rho_W|}}. \tag{36}$$

Since the change of ρ and μ causes also the variation of k_s, as presented in Eq. (31), the ultimate conclusion made from Eq. (36) is that large value of δ always lead to narrow wavenumber bandwidth. The result means that the wavenumber bandwidth of transmission gain will become inevitably small for large δ; then, we may fail in attaining high-resolution acoustic focusing. However, it is fortunate that we can find from the numerator of Eq. (35) an efficient approach of widening the bandwidth without affecting very much the surface states, which consists of reducing the slab thickness. These findings will be verified in a general manner by numerical examples shown below.

We examine transmission properties in three cases selected from Fig. 3: (1) $\rho = -990\,\text{kg/m}^3$ and $\mu = 0.5\,\text{MPa}$; (2) $\rho = -990\,\text{kg/m}^3$ and $\mu = 0.2\,\text{MPa}$; (3) $\rho = -950\,\text{kg/m}^3$ and $\mu = 0.5\,\text{MPa}$. In Figs. 4(a) and 4(b), we show exact values (solid line) of TF amplitudes for MTM thicknesses of 20 mm and 10 mm, respectively. For comparison, transmission curves calculated by approximate equation (35) are plotted by the dashed lines. The overall profile of the approximate results matches very well with the exact ones. This is very important for Eq. (36) to be used for qualitatively evaluating the influence of material parameters on the bandwidth. It can be seen in Fig. 4 that in cases of either $d = 20\,\text{mm}$ or $d = 10\,\text{mm}$, the amplitudes in the vicinity of the transmission peak have been lowered at higher values of δ. This confirms that the bandwidth becomes narrower corresponding to higher δ, as predicted by Eq. (36). However, the transmission amplitudes can be greatly enhanced in the thinner slab case ($d = 10\,\text{mm}$), then the wider bandwidth of transmission gain can be achieved. For further study, Figure 5(a) shows wavenumbers δ for various density ρ of the MTM slab with the thickness $d = 10\,\text{mm}$ and two different shear modulus $\mu = 0.5$ and 1 MPa. The modulus of the MTM is set as $\lambda + 2\mu = -\kappa_W$. Here also, the wavenumber of surface waves can be enhanced by lowering the shear modulus or increasing the contrast between $|\rho|$ and ρ_W. For three cases chosen in Fig. 5(a): (1) $\rho = -950\,\text{kg/m}^3$ and $\mu = 1\,\text{MPa}$; (2) $\rho = -930\,\text{kg/m}^3$ and $\mu = 1\,\text{MPa}$; (3) $\rho = -950\,\text{kg/m}^3$ and $\mu = 0.5\,\text{MPa}$, the corresponding transmission curves are illustrated in Fig. 5(b) and the conclusion that the bandwidth becomes narrower at higher values of δ is reinforced.

The influence of the modulus λ and μ of metamaterials on the surface states is also evaluated by fixing the MTM density $\rho = -\rho_W$. The wavenumbers δ for various modulus

$\lambda+2\mu$ of the MTM slab with the thickness $d=10$ mm are shown in Fig. 6(a) for four cases: $\mu=0.01$, 0.1, 0.5, and 1 MPa. Notice that no solutions of δ are found at $-(\lambda+2\mu)/\kappa_W<1$. In each case, δ seems to reaching a stable value when $-(\lambda+2\mu)/\kappa_W\gg 1$; therefore, the enhancement effect of δ by increasing λ is limited. In contrast, δ can be increased almost unlimitedly by the decrease of μ. It can be expected that the curve becomes flat at $\mu\to 0$, then the solid MTM model is reduced to the fluid one satisfying the perfect imaging condition. In Fig. 6(b), transmission curves are plotted in two cases: (1) $-(\lambda+2\mu)/\kappa_W=5$ and $\mu=0.1$ MPa; (2) $-(\lambda+2\mu)/\kappa_W=5$ and $\mu=1$ MPa. The conclusion about that the wavenumber bandwidth becomes narrow at high values of δ is still true in current examples. As a concluding remark, large wavenumber δ achieved by either lowering the shear modulus or increasing the contrast between $|\rho|$ and ρ_W, always leads to the transmission drop. The reduction of the MTM thickness is an important way to widen the wavenumber bandwidth of transmission gain.

In Secs. II–IV, we have investigated the theory of surface resonant states, transmission and wavenumber bandwidth of the fluid and solid MTMs. The influences of MTM parameters λ, μ, ρ on surface states, transmission and wavenumber bandwidth were clearly identified by either analytic model or numerical examples. These analyses are essential to elaborate MTM models used for high-resolution ultrasonic focusing. In Sec. V, the resolution of acoustic focusing will be analysed based on full-wave numerical simulation for solid MTMs, then the correlation between the resolution, surface states, and wavenumber bandwidth will be discussed.

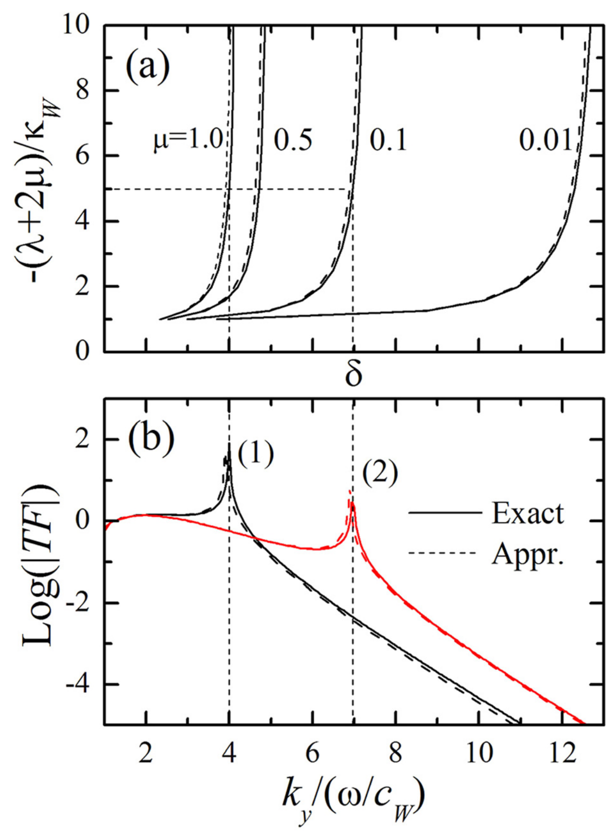

FIG. 6. (a) The normalized wavenumber δ of surface waves enabled by solid MTMs with the thickness $d=10$ mm, mass density $\rho=-\rho_W$, shear modulus $\mu=0.01$, 0.1, 0.5, and 1 MPa, and various modulus parameters $\lambda+2\mu$. (b) Amplitudes of transfer function of the solid MTMs in two selected cases: (1) $-(\lambda+2\mu)/\kappa_W=5$ and $\mu=0.1$ MPa; (2) $-(\lambda+2\mu)/\kappa_W=5$ and $\mu=1$ MPa.

V. NUMERICAL SIMULATION OF SUBWAVELENGTH ACOUSTIC FOCUSING BY SOLID MTMs

With the knowledge of surface resonant states and enhanced transmission by the solid MTM, we investigate in this section subwavelength acoustic focusing based on numerical simulations by using commercial software, COMSOL Multiphysics. In the simulation model, the solid MTM together with ambient air and water are enclosed by the perfect matched layers. A point on the left surface of the solid MTM is forced to vibrate harmonically along the direction x to act as the wave source. As an example, material parameters of the MTM slab are chosen as: $\lambda=-0.995\kappa_W$, $\mu=0.1$ MPa, $\rho=-0.995\rho_W$, and $d=10$ mm. The MTM with those parameters ensures TF amplitudes above 1 for δ ranging from 1 to 6. The normalized pressure distribution for the air/MTM/water system is shown in Fig. 7(a). As the evidence of existence of excited surface waves, bright spots are clearly observed and appear periodically along the MTM-Water interface. Since the impedance of the longitudinal mode in the MTM is matched very well to that of the water, wave energy carried by propagating waves is mostly transported into the water region, and the sound focusing is formed due to the negative refractive index of the MTM. Energy leakage to the air region is very low due to the great impedance mismatching between the air and MTM. While for the water/MTM/water system as illustrated in Fig. 7(b), energy can also flow into the back water medium. The refractive index of the MTM is equal in magnitude to that of water; that means the focal distance d_F is equal to the MTM thickness. We therefore examine the focusing capability in the image line located at $d_F=d$ by plotting the lateral distribution of pressure amplitude, as illustrated in Fig. 7(c). The result clearly demonstrates the sub-diffraction-limited hyperfocusing with the spatial resolution $0.2\lambda_W$ and $0.12\lambda_W$ corresponding, respectively, to the air and water back mediums, which is defined as full width at half maximum (FWHM) of the transmission peak measured at the basis of the peak.[27] The presence of the superfocusing emphasizes the role of evanescent wave enhancement for the formation of a tight focusing spot. It is also demonstrated that the MTM superlens with surface attached source is robust against the change of the back medium. Further results will be shown below for the air/MTM/water system regarding how fine resolution is associated to the wide wavenumber bandwidth of transmission gain.

Figure 8 shows the FWHM measured at $d_F=d$ for various MTM thickness corresponding to the following material parameters $\lambda=-0.995\kappa_W$, $\mu=0.02$ MPa, and $\rho=-0.995\rho_W$. The wavenumber bandwidth of transmission gain is marked by the shaded region in the k_y space where the amplitude of the transfer function TF is over the unity. The fact that has also been predicted in Sec. IV is that the bandwidth becomes narrower gradually as the MTM thickness increases. As a consequence, the resolution becomes worse smoothly. This emphasizes the importance of widening transmission bandwidth in high-resolution acoustic focusing. To get further insights into the role of the shear modulus in acoustic hyperfocusing, we show in Fig. 9 the FWHM as a function of the shear modulus for the same MTMs used in Fig. 8 with two different thicknesses 2 mm and 5 mm. The result shows that it is not straightforward to achieve high resolution by lowering shear modulus because of the inversely proportional relationship between δ and wavenumber bandwidth, as indicated in Eq. (36). However, reliable high-resolution acoustic focusing can still be obtained, although a small fluctuation in the resolution is observed. It is worth to highlight here that the best resolution achieved in the case of $\mu = 0.01$ MPa and $d = 2$ mm is up to $\lambda_W/28.4$.

We now have clearly identified the effect of metamaterial parameters on surface states, transmission, wavenumber

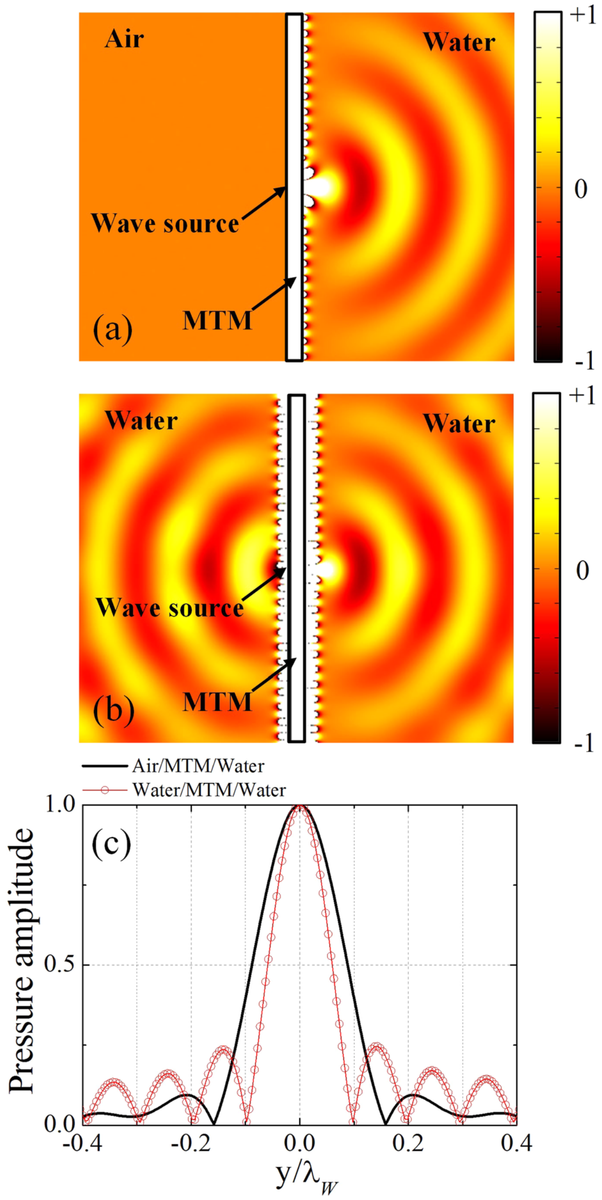

FIG. 7. Normalized pressure distributions in (a) air/MTM/water and (b) water/MTM/water systems where the MTM slab with the set of parameters $\lambda = -0.995\kappa_W$, $\mu = 0.1$ MPa, $\rho = -0.995\rho_W$, and $d = 10$ mm is excited by surface attached sources. (c) The lateral distribution of pressure amplitude in the image line located at $x = d$ for both systems.

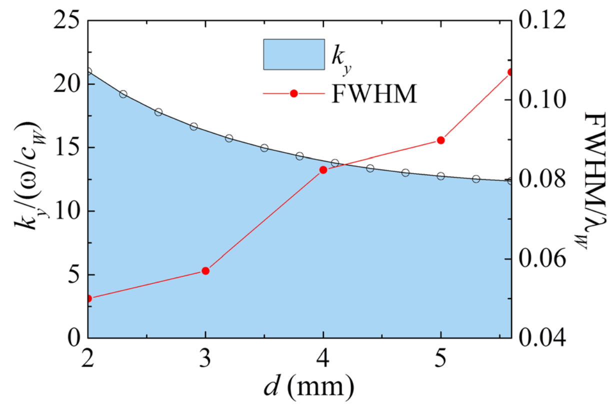

FIG. 8. The FWHM measured at $d_F = d$ for various MTM thickness corresponding to the following material parameters $\lambda = -0.995\kappa_W$, $\mu = 0.02$ MPa, and $\rho = -0.995\rho_W$. The shaded region marks the k_y space where the amplitude of the transfer function is over the unity.

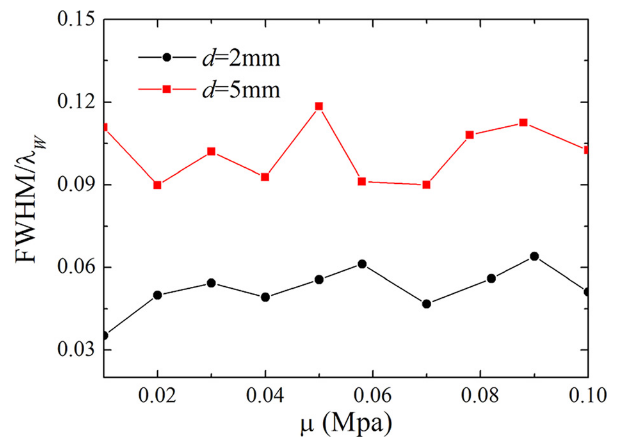

FIG. 9. The FWHM as a function of the shear modulus for the same MTMs used in Fig. 8 with two different thicknesses 2 mm and 5 mm.

bandwidth, and resolution of focusing. Based on the concept developed above, the optimum effective physical parameters of solid MTMs can be designed for sub-diffraction-limited resolution of acoustic focusing. The study then opens an exciting way to design acoustic metamaterials for ultrasonic focused imaging.

VI. CONCLUSION

We have studied acoustic focusing with sub-diffraction-limited resolution induced by surface resonant states of solid MTMs. The proposed model based on the solid MTM excited by surface attached source is robust against the change of the back medium due to the fact that the transfer function is unrelated to physical properties of the incident region. We have found that solid MTMs with small shear modulus or small mass density can produce large wave vectors of surface waves, which results in inevitably narrow wavenumber bandwidth. It is important to find that the MTM thickness is an essential and almost independent parameter for enlarging wavenumber bandwidth of transmission gain of evanescent waves. Above conclusions are obtained based on analytic models under LSM approximation and verified in a general manner by numerical examples. The research conducted in this work will be helpful for designing effective physical parameters of solid MTMs for high resolution acoustic focusing.

ACKNOWLEDGMENTS

M.B.A. and M.O. would like to thank "La Région Lorraine" for its financial support. X.Z. acknowledges supports from the National Natural Science Foundation of China (Grant Nos. 11172038 and 11221202) and Program for New Century Excellent Talents in University (Grant No. NCET-11-0794).

[1]L. Fok, M. Ambati, and X. Zhang, MRS Bull. **33**, 931–934 (2008).
[2]M.-H. Lu, L. Feng, and Y.-F. Chen, Mater. Today **12**(12), 34–42 (2009).
[3]S. Zhang, L. Yin, and N. Fang, Phys. Rev. Lett. **102**(19), 194301 (2009).
[4]J. Li, L. Fok, X. Yin, G. Bartal, and X. Zhang, Nature Mater. **8**(12), 931–934 (2009).
[5]J. Zhu, J. Christensen, J. Jung, L. Martin-Moreno, X. Yin, L. Fok, X. Zhang, and F. J. Garcia-Vidal, Nat. Phys. **7**(1), 52–55 (2011).
[6]X. Ao and C. T. Chan, Phys. Rev. E **77**(2), 025601 (2008).
[7]Y. Cheng, C. Zhou, Q. Wei, D. Wu, and X. Liu, Appl. Phys. Lett. **103**(22), 224104 (2013).
[8]H. Jia, M. Ke, R. Hao, Y. Ye, F. Liu, and Z. Liu, Appl. Phys. Lett. **97**(17), 173507 (2010).
[9]A. Liu, X. Zhou, G. Huang, and G. Hu, J. Acoust. Soc. Am. **132**(4), 2800–2806 (2012).
[10]X. Zhou and G. Hu, Appl. Phys. Lett. **98**(26), 263510 (2011).
[11]J. Christensen and F. J. García de Abajo, Appl. Phys. Lett. **97**(16), 164103 (2010).
[12]D. Lu and Z. Liu, Nat. Commun. **3**, 1205 (2012).
[13]J. B. Pendry, Phys. Rev. Lett. **85**(18), 3966–3969 (2000).
[14]X. Zhang and Z. Liu, Nature Mater. **7**(6), 435–441 (2008).
[15]M. Ambati, N. Fang, C. Sun, and X. Zhang, Phys. Rev. B **75**(19), 195447 (2007).
[16]S. H. Lee, C. M. Park, Y. M. Seo, Z. G. Wang, and C. K. Kim, Phys. Rev. Lett. **104**(5), 054301 (2010).
[17]C. Park, J. Park, S. Lee, Y. Seo, C. Kim, and S. Lee, Phys. Rev. Lett. **107**(19), 194301 (2011).
[18]W. Akl and A. Baz, J. Appl. Phys. **111**(4), 044505 (2012).
[19]J. Christensen and F. J. G. de Abajo, Phys. Rev. Lett. **108**(12), 124301 (2012).
[20]Z. Yang, J. Mei, M. Yang, N. Chan, and P. Sheng, Phys. Rev. Lett. **101**(20), 204301 (2008).
[21]Z. Liu, X. Zhang, Y. Mao, Y. Y. Zhu, Z. Yang, C. T. Chan, and P. Sheng, Science **289**(5485), 1734–1736 (2000).
[22]K. Deng, Y. Ding, Z. He, H. Zhao, J. Shi, and Z. Liu, J. Appl. Phys. **105**(12), 124909 (2009).
[23]X. N. Liu, G. K. Hu, G. L. Huang, and C. T. Sun, Appl. Phys. Lett. **98**(25), 251907 (2011).
[24]Y. Lai, Y. Wu, P. Sheng, and Z. Q. Zhang, Nature Mater. **10**(8), 620–624 (2011).
[25]R. Zhu, X. N. Liu, G. L. Huang, H. H. Huang, and C. T. Sun, Phys. Rev. B **86**(14), 144307 (2012).
[26]R. Zhu, X. N. Liu, G. K. Hu, C. T. Sun, and G. L. Huang, J. Sound Vib. **333**(10), 2759–2773 (2014).
[27]A. Sukhovich, L. Jing, and J. H. Page, Phys. Rev. B **77**(1), 014301 (2008).